PRE-PRINT ARTICLE

COPYRIGHT BY COMPOSITES THEORY AND PRACTICE JOURNAL

ISSN: 2299-128X

Lightweight, multi-layer structures based on aluminium foam for critical infrastructure shielding applications

Jaroslav Kováčik[1] (0000-0002-6970-0406), Joanna Kulasa[2](0000-0001-5036-4847), Anna Brudny[2] (0000-0001-6353-207X)

[1] Institute of Materials and Machine Mechanics SAS, Dúbravská cesta 9/6319, 845 13 Bratislava, Slovak Republic

[2] Łukasiewicz Research Network – Institute of Non-Ferrous Metals, Sowińskiego 5, 44-100 Gliwice, Poland

Correspondence: anna.brudny@imn.lukasiewicz.gov.pl

https://doi.org/10.62753/ctp.2026.01.4.4

Abstract

The aim of the study is to develop a lightweight, multi-layer sandwich structure based on aluminium foam that will protect against both projectile impact and the pressure wave generated by an explosion, with applications in critical infrastructure protection in mind, including public facilities. The developed shield is a sandwich structure reinforced with Al_2O_3 ceramic plates, stainless steel mesh, aluminium foam and Kevlar. The adopted concept aimed to combine a high energy absorption capacity with the lowest possible total system weight. As part of the work, modified compression tests were conducted utilising a pin simulating 7.62 mm calibre ammunition, as well as 3-point bending tests to evaluate energy absorption and mechanical properties. Analysis of the obtained results demonstrated that the use of a ceramic layer and steel mesh inside the aluminium foam significantly increased the sandwich structure's resistance to compression and bending, particularly at maximum loads. Preliminary ballistic tests with 7.62×51 mm NATO ammunition showed promising results. It was found that while the sandwich structure itself exhibits favourable mechanical properties, the thickness of the employed ceramic layer was insufficient to stop or disrupt a projectile when the sandwich structure was used alone. A multi-layer sandwich structure in conjunction with 24 mm thick EN AW7075 back plates resulted in penetration of the sandwich structure, while not completely penetrating the armour. When fired at a 30° angle, the plate was merely scratched without any significant damage (ricochet), confirming the validity of the multi-layered protection system concept.

Keywords: aluminium foams, ballistic shields, infrastructure protection, multi-layered materials, sandwich structures

Introduction

Modern countries face increasingly complex challenges related to the safety of civilian populations and the protection of critical infrastructure [1], such as airports, railway and subway stations, hospitals, schools, shopping malls, stadiums, other high-traffic spaces, also including critical industries, oil refineries, supply chains, warehouses, telecommunications, in addition to water supply systems as well as electric production and supply systems.

PRE-PRINT ARTICLE
COPYRIGHT BY COMPOSITES THEORY AND PRACTICE JOURNAL
ISSN: 2299-128X

Criminal, terrorist, sabotage-related, or accidental events and civilian targets during war can endanger human life, disrupt the functioning of public institutions, and destabilise essential national systems. These facilities, along with human lives, can be threatened by attacks by bombs or drones. [2]. The Global Terrorism Database (GTD) analysis (1970–2020) identified 7,813 attacks on critical infrastructure [3]. These attacks resulted in 1,917 deaths and 1,377 injuries, in addition to high economic costs that are much more difficult to estimate due to the long-term effects beyond immediate damages.

The majority of terrorist attacks have been conducted traditionally by bombs or improvised explosive devices, having more or less powerful blast and fragmentation effects [2]. Today, there is a very real possibility of employing first-person view drones (FPV), as well as loitering munitions utilising unmanned aerial vehicles (UAV); both of them could be used in peace as well. While FPV drones have a relatively short range, loitering munitions (e.g. Shahed and Geran) can reach targets 2500 km away and have been successfully used against critical infrastructures during the war in Ukraine.

Critical infrastructure is currently protected from drone/loitering munitions by various means like soft and hard-kill [4]. A typical soft-kill measure is electronic warfare in the form of various types of jammers, some effective against small and medium drones, usually aimed at disrupting their navigation or communication systems. Hard-kill methods consist in shooting them down with missiles, guns, lasers or other ramming drones. These means are either overly expensive (missiles) or have a relatively short range, especially when swarms of drones are used.

To protect critical infrastructures during an attack, it is necessary to provide blast overpressure protection, kinetic energy projectiles/fragmentation, as well as blast-fragmentation protection, preferably in one single panel [5]. Addressing these threats requires the development of advanced, lightweight, and cost-effective protective technologies that can be deployed in both civilian and public administration sectors. Currently, passive mitigation systems utilise the structural properties built into the design of the system [6]. This makes the passive system simpler and eliminates any reaction time between the event and the response. Common techniques employed in passive systems include impedance mismatching, sacrificial cladding, blast deflection, in addition to blast and shockwave disruption.

Structural materials employed in passive systems are usually ultra-high-performance concrete (UHPC) and fibre-reinforced concrete; high-strength structural steel [7]; and advanced composite materials, such as fibre-reinforced polymers (FRP) made with carbon, aramid, or glass fibres. Laminated glass containing strong polymeric interlayers, energy-absorbing metal foams, sandwich panels with cellular cores, and heavy masonry units filled with grout or sand are also utilised [8].

Among the most effective energy absorbing materials today are various types of metallic foams. One of the most ubiquitous foam metallic materials is based on aluminium and aluminium alloy foams [9-14]. In 2003, Jerz et al. [15] investigated the possibility of applying aluminium foam reinforced with expanded stainless-steel sheet in the design of future military vehicles [16]. They stated that the foam itself does not have the

PRE-PRINT ARTICLE
COPYRIGHT BY COMPOSITES THEORY AND PRACTICE JOURNAL
ISSN: 2299-128X

ability to absorb the energy of a projectile or splinter because the projectile loading is realised on a very small area. The combination of metallic foam with other advanced materials was proposed.

The research group of A. Rabiei [17, 18] observed that owing to its lightweight and high impact energy absorption capabilities, composite metal foam produced by the powder metallurgy technique could be used as a bullet kinetic energy absorber interlayer, with aluminium 7075 or KevlarTM panels as back plates with a total armour thickness less than 25 mm. It would also be suitable in terms of vibration damping and electromagnetic shielding.

The objective of the present work is to investigate the possibility of developing innovative ballistic shields based on aluminium foams to protect personnel, critical infrastructure and vehicles against bullets, shrapnel and other direct threats. The sandwich structure shields, consisting of aluminium foams reinforced with foamed-in steel mesh, an alumina ceramic plate or both, were produced. As a cover sheet, Kevlar textile was glued onto the designed sandwich layers. Observation of the structure, compression and 3-point bending tests of the prepared sandwich structures were carried out. Finally, preliminary ballistic tests were performed in real conditions with 7.62 mm calibre munition. Their modularity and adaptability make them suitable for protective barriers, mobile shielding systems, as well as the structural reinforcement of buildings or vehicles.

Experimental part

Materials

Reinforced foams were prepared in one-step foaming. An aluminium foam precursor with a stainless steel mesh/alumina ceramic plate were inserted into the mould together. During foam expansion, the properly positioned reinforcements were infiltrated/foamed around with the molten material. For preparation of the sandwich structures, the prepared aluminium foam samples and/or composite aluminium foam samples with the incorporated steel mesh/ceramic plate were glued together and also covered with Kevlar fabric by means of methacrylic adhesive glue.

The aluminium foam precursor composition was AlSi10 + 0.4 wt% TiH_2. It was prepared by direct hot extrusion of the CIPed powder mixture at 450°C (Hydro Extrusion Slovakia a.s., Žiar nad Hronom, Slovakia). The stainless steel mesh (areal weight of 3400 g/m^2) had a diamond shape (6 mm x 3 mm), was 0.5 mm thick, and the width at the junction was 1 mm (Perfora s.r.o., Trnava, Slovakia). It was made of X5CrNi 18-10 stainless steel with the composition Cr 17-19.5%, Ni 8-10.5, C < 0.07%, which is austenitic Cr-Ni stainless steel with corrosion resistance to most oxidising acids and salt spray.

The alumina ceramic was cut from ceramic plates 150 mm x 200 mm x 0.7 mm made by sintering fine alumina powders (Effpower AB, Vikmanshyttan, Sweden). The residual porosity of the ceramic was around 20% according to mercury intrusion porosimetry measurements (Quantachrome Poremaster 60GT, SAS, Bratislava, Slovakia). Porous alumina was originally chosen to improve the mechanical bond with the aluminium foam during the foaming process. Alumina plates of different sizes (38 mm x 38 mm, 190 mm x 38 mm, 190 mm x

PRE-PRINT ARTICLE
COPYRIGHT BY COMPOSITES THEORY AND PRACTICE JOURNAL
ISSN: 2299-128X

90 mm) according to the mould size and testing designation were diamond cut with a band saw. The areal weight of the employed ceramic was around 2790 g/m^2.

For the experiments, Kevlar fabric with an areal weight of 300 g/m^2, model: KEV300 was used. Kevlar fabric (SIA Kompozītmateriāli, Rīga, Latvia) is significantly stronger than steel, with a tensile strength of 2.4 GPa and elongation at break 4% [19]. The Kevlar was cut with scissors to the required size. It was then glued to/into the composite foam samples according to the designed layer structure. Melkib MMA Power 10 400 ml beige 2-component methacrylic adhesive was utilised (Melkib Klus Raczek Limited Partnership, Cieszyn, Poland). This two-component methacrylic adhesive is characterised by a very high Shore hardness of 78D, and the tensile shear strength for paired aluminium and plastic material is 15 N/mm^2 [20]. Bonding of the sandwich structure layers was performed with a preparation time of 8 - 16 min., binding time 30 - 45 min., and time to reach final strength 24 h.

Foaming was carried out in an electric resistance furnace at the temperature of 680°C for 10 minutes. Two steel moulds were employed: a small one with inner dimensions of 40 mm x 40 mm x 40 mm and a large one with inner dimensions of 200 mm x 100 mm x 10 mm. In the case of the reinforced foam, the desired reinforcement was placed into the mould with the foaming precursor. When the mould reached a temperature just above the melting point of the used alloy, the blowing agent decomposed and released hydrogen, which swelled the molten aluminium into a porous foam. After 10 minutes, the mould was taken out of the furnace and air cooled to stabilize the cellular structure.

The final density of the pure foams varied in the range of 0.53 – 0.69 g.cm^{-3} for the foams produced in a small mould, and in the range of 0.64 – 0.74 g.cm^{-3} for the reinforced foams prepared in a small mould. In the large mould, the foam densities were in the range of 0.49 – 0.81 g.cm^{-3} for bending, and in the range of 0.72 – 0.92 g.cm^{-3} for ballistic tests.

The pure foam density was ascertained from the measured values of weight and sample geometry. In the case of the reinforced foams, the density was calculated identically. The foam weight was determined as the difference between the weight of the reinforced foam and the weight of the used reinforcement before foaming. The conservation of mass is expected for reinforcements.

Research methodology

Compression tests were carried out on a Zwick/Roel 100kN universal testing machine at a constant loading rate of 30 MPa/s with a new pin design (see Fig. 1) to imitate the impact testing of 7.62 mm ammunition. Prior to the compression experiments, the pin was firmly pressed to the foam/reinforced foam/sandwich structure surface at a small load. The compression tests were then carried out to full penetration of the pin into the sample.

PRE-PRINT ARTICLE
COPYRIGHT BY COMPOSITES THEORY AND PRACTICE JOURNAL
ISSN: 2299-128X

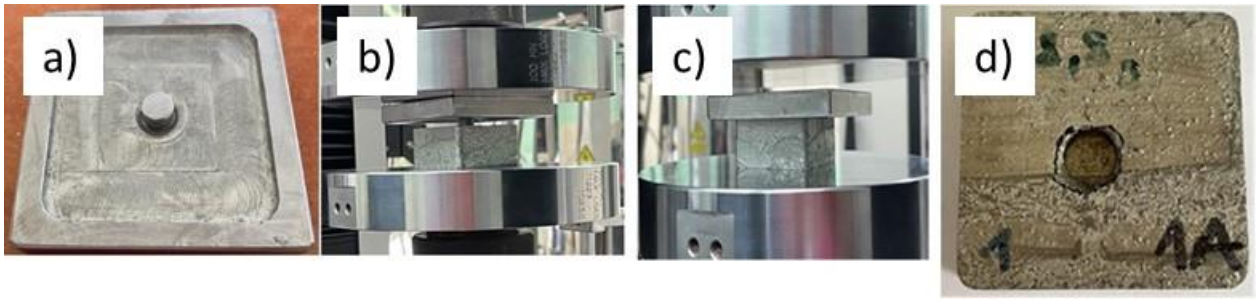

Fig. 1. Newly designed upper plate for compression tests with pin ϕ 7.7 mm and length of 5.2 mm (a). Compression test set-up at beginning (b) and end of test (c). Top surface of sample after test (d).

Bending tests were conducted by means of an INSTRON 600DX 600 kN testing machine. For the bending tests, a 3-point bending test configuration was chosen with a span of 50 mm to imitate the ballistic test conditions (Fig. 2). The diameter of the support and pin was 5 mm. 3-point bending was performed with a constant ram speed of 10 mm/min. Sandwich structures were prepared from foams with reinforcements glued together with Kevlar.

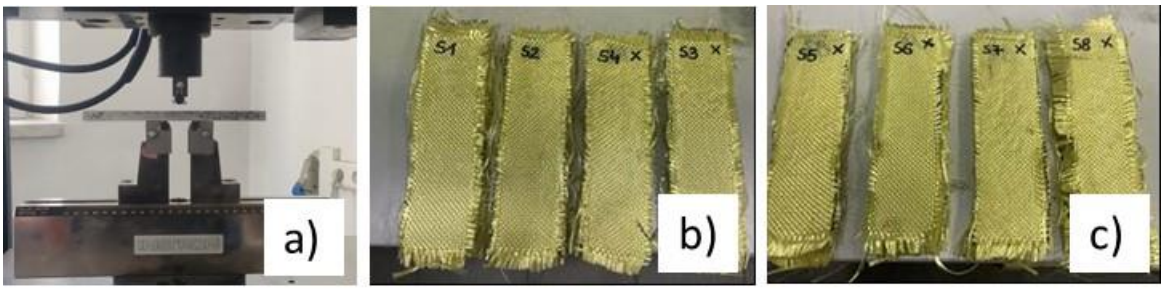

Fig. 2. 3-point bending test stand: a) aluminium foam before bending: 200 x 49.5 x 10 mm, density 0.68 g/cm^3, and sandwich structure foam samples before bending test (b, c). X marks upper side of sample during bending.

The ballistic tests were carried out at The Military Institute of Armoured and Automotive Technology (WITPiS), Sulejówek, Poland. Based on the bending test results, it was proposed to work with the following combination of sandwich structure layers: Kevlar-glue-stainless steel mesh + foam-glue-Kevlar–glue-foam+ ceramic plate + stainless steel mesh-glue-Kevlar (Fig. 3). The areal weight of the sandwich structure sample was around 24000 g/m^2. For a complex, non-uniform sandwich structure, the areal weight was measured by dividing the total weight by the total surface area of the sandwich structure.

The sandwich structure samples were mounted on the stand at a distance of 20 mm from a 24 mm thick aluminium plate EN AW 7075 (AlZn5.5MgCu) in the T651 state (Fig.3). The shots were performed at shot angles of 90° and 30° to the sample surface. NATO ammunition calibre with a lead core of 7.62 x 51 mm had the following properties: weight 10–11 g, speed 790 – 860 m/s and energy 3.47 – 3.59 J depending on the

PRE-PRINT ARTICLE
COPYRIGHT BY COMPOSITES THEORY AND PRACTICE JOURNAL
ISSN: 2299-128X

variations of ammunition. The tests were performed at 15°C and 55% humidity. The amount of used gunpowder was calculated to have an impact speed of 833 ± 20 m/s after 12 m of flight of the bullet.

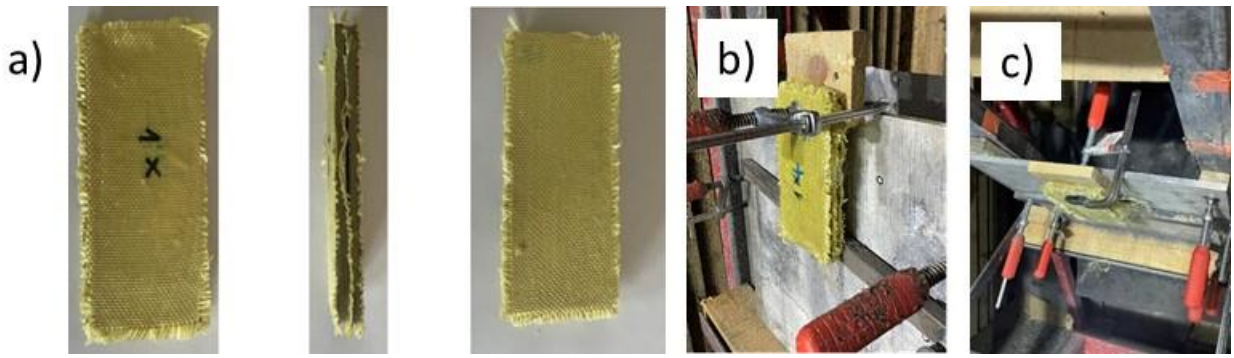

Fig. 3. a) Sandwich structure sample No. 1 used for preliminary ballistic tests with 7.62×51 mm NATO ammunition. Side with mesh and ceramic facing incoming bullet was marked as X, areal weight 24200 g/m^2. Mounting of samples for shots performed at shot angles: b) 90° and c) 30°.

Structural investigations were performed on a Keyence VHX-7000 series high-resolution 4k light microscope. Investigation of the foams' structural changes after the mechanical tests was conducted by X-ray computed tomography (CT). The X-ray micro tomography device Phoenix Nanotom is designated for non-destructive analysis of the internal structure of materials.

Results and discussion

At first, compression tests with a pin were performed on foam and reinforced foam samples with mesh, ceramic and glued ceramic. The stress-strain curve indicates that, in comparison to the usual aluminium foam stress-strain curve, only elastic-plastic and plateau regions are observed with the pin. The densification region is missing [14]. The XRD observations indicate that the deformed foam volume is pressed into the foam structure just below the pin (see red arrow in Fig. 4). There is still foam below the pin area that could be collapsed; therefore, the foam compression response is still in the plateau region, even when the whole pin length was pressed into the sample, i.e. at strain = 1.

The stress-strain curves confirmed that the compression strength, plateau stress and energy absorption of the composites improved in comparison with simple foam (Fig. 4, Table 1). However, different deformation results were observed according to the applied reinforcing elements (Fig. 5). The energy absorption of the investigated samples is the area under the stress-strain curve. From Fig. 4 the corresponding energy absorption areas of foam and foam + ceramics are very similar. The foam + mesh significantly improves the energy absorption and the foam + glued ceramic has the best value.

PRE-PRINT ARTICLE

COPYRIGHT BY COMPOSITES THEORY AND PRACTICE JOURNAL

ISSN: 2299-128X

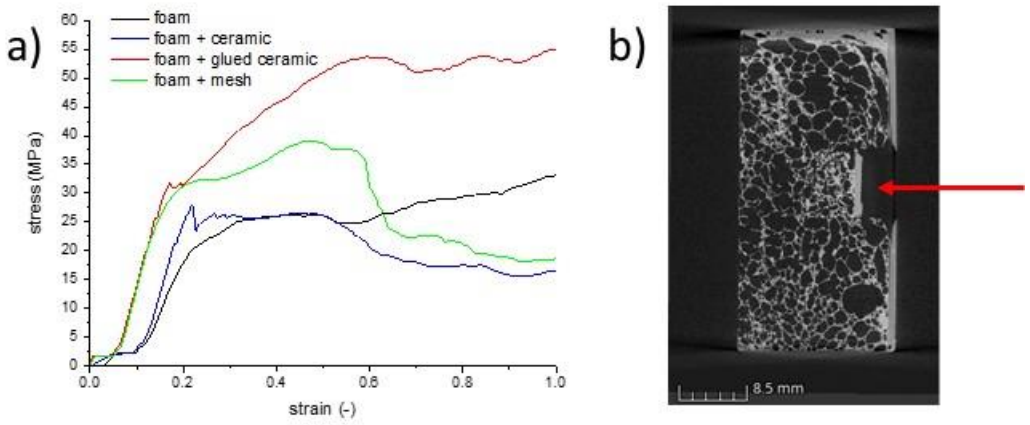

Fig. 4. a) Stress-strain compression response with pin: simple foam (1A, 0.61 g.cm^{-3}), foam with ceramic (6B, 0.63 g.cm^{-3}), foam with mesh (8B, 0.58 g.cm^{-3}), and foam with glued ceramic (8A, 0.58 g.cm^{-3}) broken apart during compression test (see Fig. 5). b) X-ray computed tomography (CT) of foam with ceramic sample structure after test.

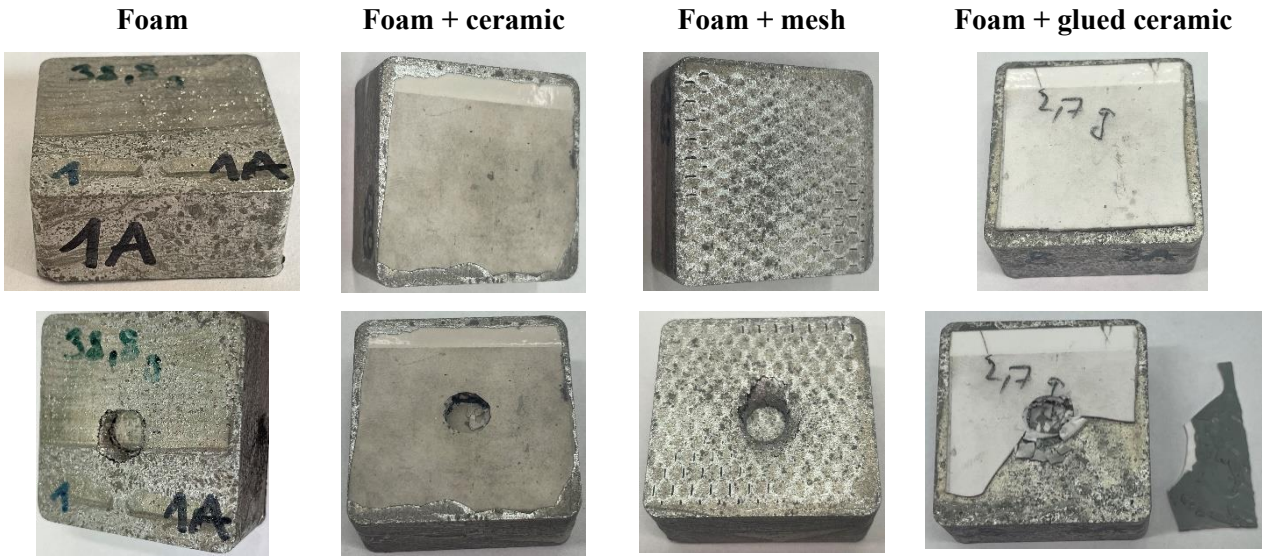

Fig. 5. Samples prior to (top) and after compression tests with pin (bottom): simple foam (0.61 g.cm^{-3}), foam with ceramic (0.63 g.cm^{-3}), foam with mesh (0.58 g.cm^{-3}), and foam with glued ceramic (0.58 g.cm^{-3}) broken apart during test.

Table 1. Compression test results on foam and reinforced foams with single reinforcements.

Sample	Reinforcement	Foam density	Compression strength	Plateau stress	Energy absorption at 100% strain
No		[g.cm^{-3}]	[MPa]	[MPa]	[MJ/m^3]
1A	only foam	0.61	26.1	25.7	22.7
6B	ceramic	0.63	27.9	26.2	18.6
8A	glued ceramic	0.58	55.1	45.7	42.2
8B	mesh	0.58	38.9	35.8	25.6

PRE-PRINT ARTICLE
COPYRIGHT BY COMPOSITES THEORY AND PRACTICE JOURNAL
ISSN: 2299-128X

When a ceramic plate with 20% porosity was incorporated into the aluminium foam, almost no reaction was observed between the foam and alumina (Fig. 6a). The porosity does not improve the mechanical bonding between foam and alumina ceramic either. The ceramic plate is only held in place by foam that overflows the plate edges in the mould.

The stiffness and strength of the ceramic are higher than those of the foam. When the bending strength of the ceramic is reached, the ceramic under the pin breaks and the compression stress drops in several sharp steps as a consequence of ceramic delamination (Fig. 4a). The stress is now controlled only by the foam stress-strain compression response as can be seen in Fig. 4. The created hole is almost circular with visible ceramic debris and its diameter corresponds to the pin diameter of 7.7 mm (Fig. 6b).

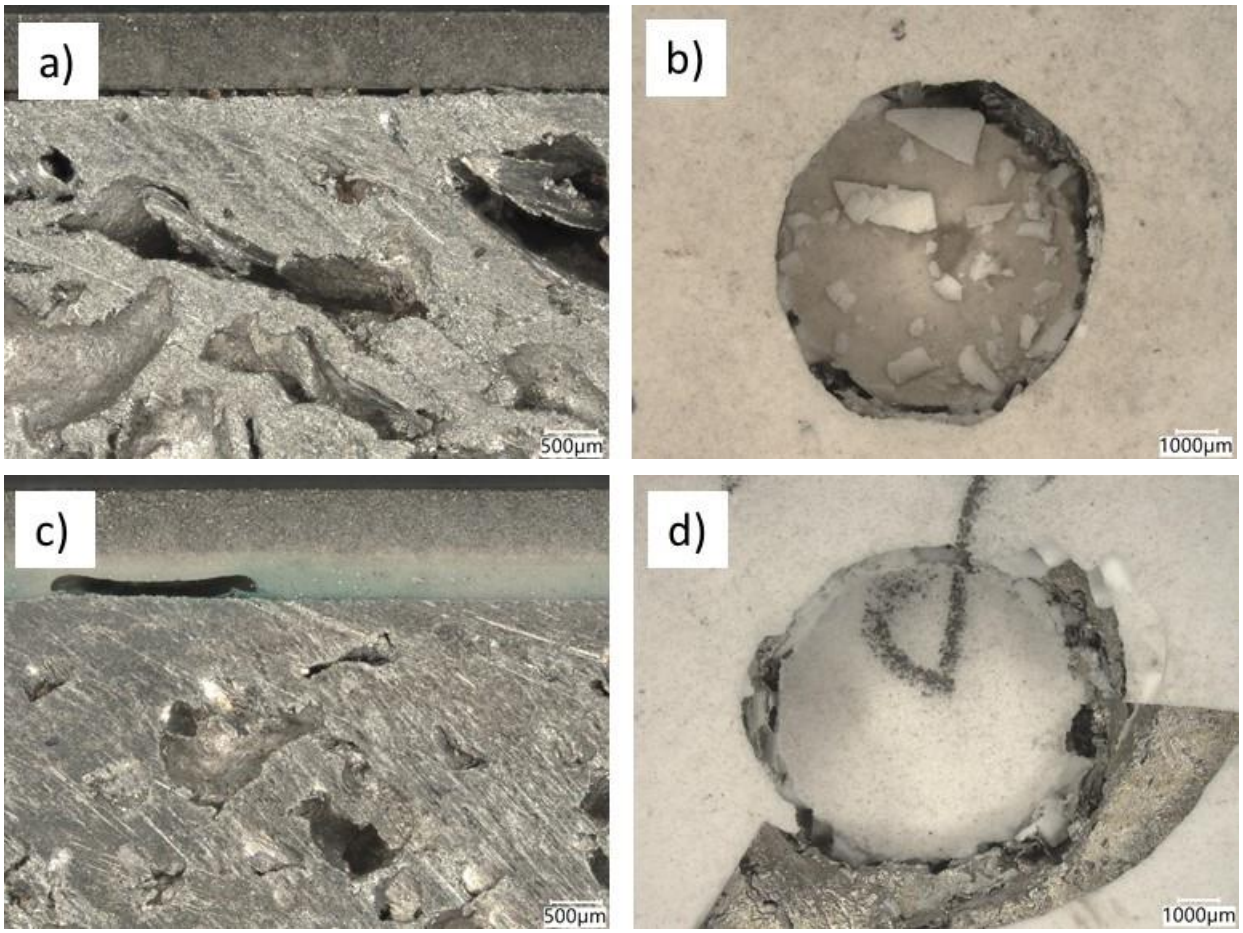

PRE-PRINT ARTICLE
COPYRIGHT BY COMPOSITES THEORY AND PRACTICE JOURNAL
ISSN: 2299-128X

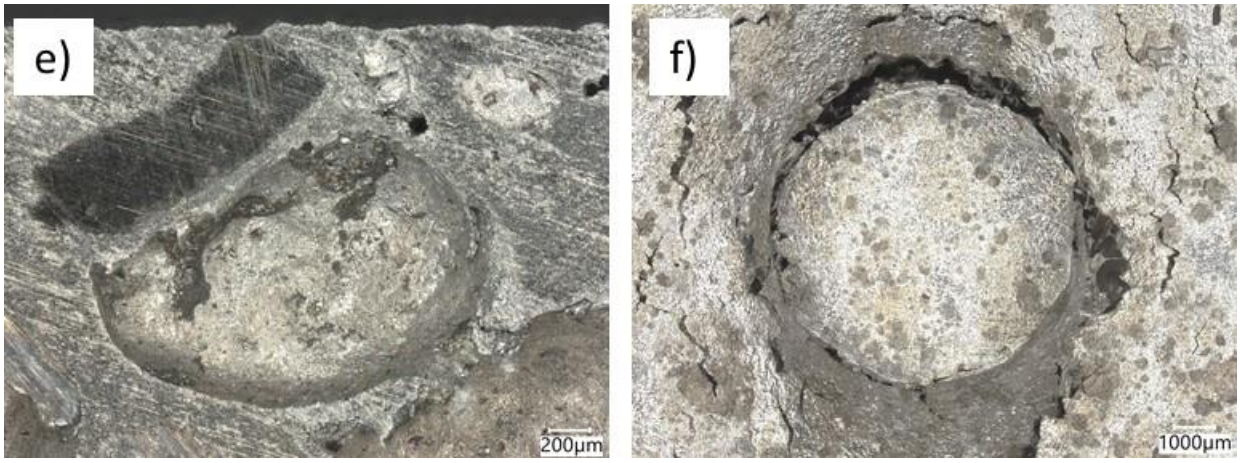

Fig. 6. Cross section (left) and detail of area under pin (right): a) and b) foam with ceramic (6B, 0.63 g.cm^{-3}), c) and d) foam with glued ceramic (8A, 0.58 g.cm^{-3}), e) and f) foam with mesh (8B, 0.58 g.cm^{-3}). Light microscope.

When ceramic was glued onto the surface of the aluminium foam, its adhesion to the foam substrate significantly improved (Fig. 6c). Therefore, the stiffness and strength of the foam with the glued ceramic are higher than those of the foam + ceramic (Fig. 4a). This is a result of a significantly larger transfer of force to the foam via the glue layer. The hole diameter is larger and is around 9 mm in this case – compare Figs. 6b and 6d. It indicates that after gluing, the created cone below the ceramic is significantly enlarged in comparison with the directly foamed ceramic (diameter of cone 7.7 mm). Unfortunately, as shown in Figs. 5 and 6d, there is significant delamination of the ceramic from the foam surface after the compression test. A large portion of the sample is without a ceramic cover. This is a problem for ballistic protection against multiple hits to the same place.

PRE-PRINT ARTICLE

COPYRIGHT BY COMPOSITES THEORY AND PRACTICE JOURNAL

ISSN: 2299-128X

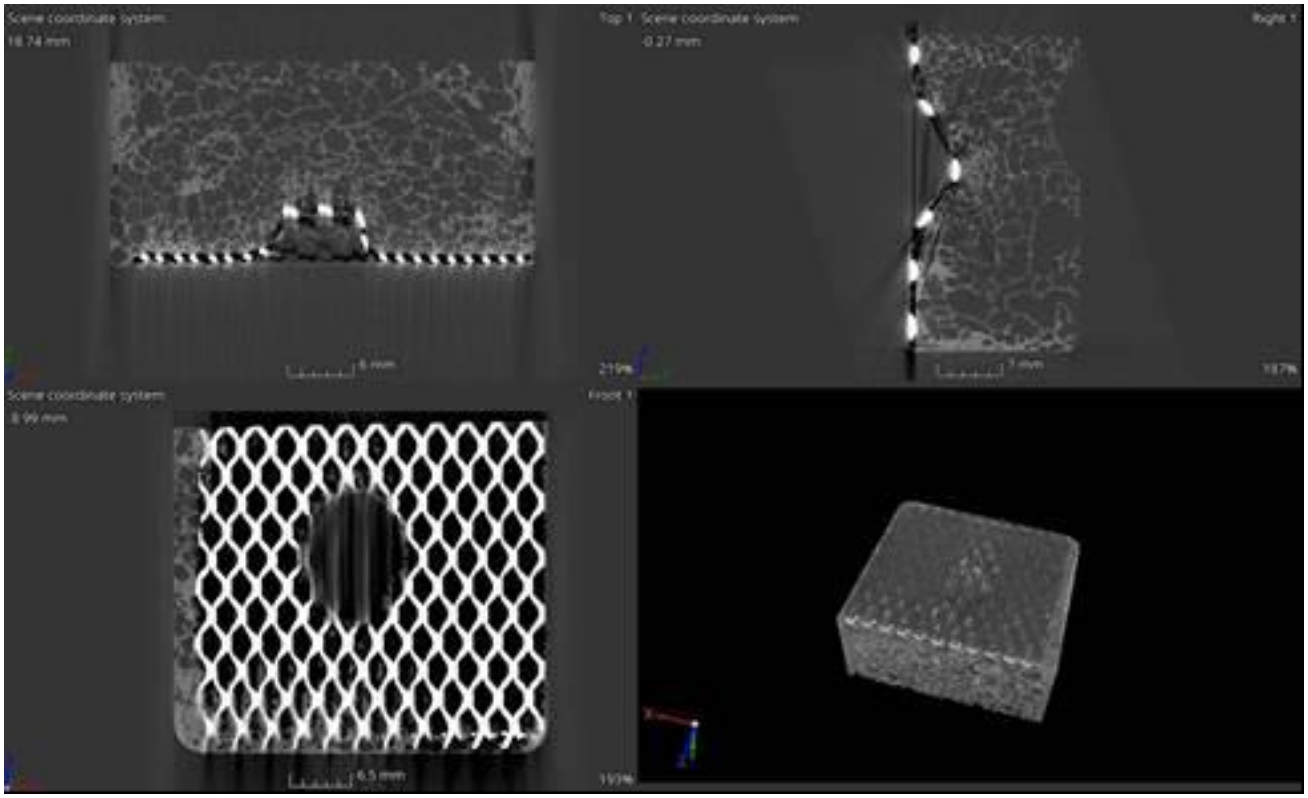

Fig. 7. Microstructure of foam with mesh (8B, 0.58 g.cm^{-3}) after compression in chosen X, Y, and Z planes, and overall picture created by X-ray computed tomography (CT).

When the stainless steel mesh infiltrated by the foam, no voids were observed between the mesh and aluminium (Fig. 6e). According to previous observations [21], the stainless steel mesh reacts with the AlSi10 foam via diffusion bonding of elements between the mesh and the foam – Cr and Si are the main diffusing elements. The light grey interface between the mesh and foam in Fig. 6e confirm this diffusion bonding in the investigated composite samples. Therefore, the stiffness and strength of the foam with the mesh are higher than those of the foam + ceramic (Fig. 4a). This is a result of a significantly larger transfer of force to the foam via the mesh geometry. The hole diameter at the bottom is around 7.8 mm, but near the surface it is significantly larger – up to 13 mm (Figs. 6f and 7). The mesh deformation patterns are either rectangular or parabolic, depending on the investigated perpendicular planes.

To improve the ballistic response of the reinforced foams, a combined layer of stainless-steel mesh and ceramic was proposed to avoid the above-mentioned problem of the ceramic falling apart. Therefore, the combinations of stainless-steel mesh with ceramic incorporated into the foam during foaming were further tested: ceramic on steel mesh or steel mesh on ceramic. Finally, on the top surface of the prepared samples, Kevlar was also glued (sandwich structures).

PRE-PRINT ARTICLE
COPYRIGHT BY COMPOSITES THEORY AND PRACTICE JOURNAL
ISSN: 2299-128X

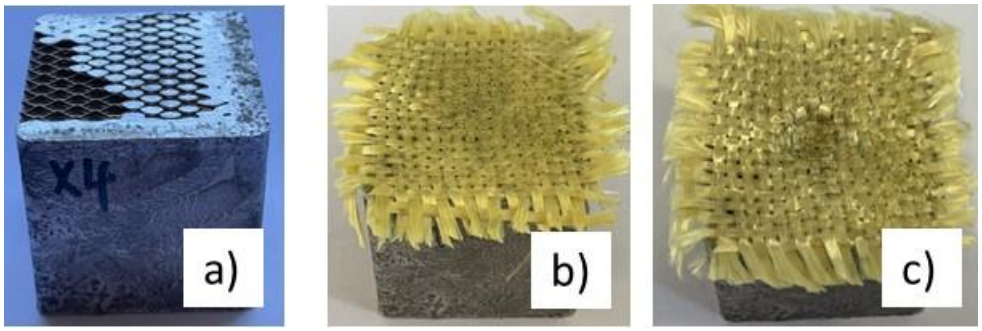

Fig. 8. a) Reinforced foam sample X4 after foaming with mesh and ceramic, b) sandwich structure after gluing Kevlar layer on X4 and c) after compression test with pin: foam core density 0.70 g.cm^{-3}.

Table 2. Compression test results for foam composites/sandwich structure with mixed reinforcements and glued Kevlar layer.

Sample No	Composite layer/sandwich structure	Foam density	Compression strength	Plateau stress	Energy absorption at 100% strain
		[g.cm^{-3}]	[MPa]	[MPa]	[MJ/m^3]
1`	ceramic	0.67	22.8	22.3	18.4
4`	ceramic + Kevlar	0.68	24.7	20.5	17.5
X2	mesh + ceramic	0.72	70.8	64.5	45.8
X4	**mesh + ceramic + Kevlar**	0.70	107.7	69.1	**73.4**
S2	mesh	0.74	79.2	63.6	55.4
Y1	ceramic + mesh	0.73	67.3	48.5	47.7

The stress-strain response of the sandwich structure with Kevlar glued on the ceramic layer is almost similar to the composite sample without Kevlar (Table 2). In contrast, the sandwich structure made of reinforced foam containing mesh + ceramic and glued Kevlar exhibits the best compression strength, plateau stress and energy absorption at 100% strain among all the samples (Table 2).

As the sandwich structures with mesh + ceramic in foam and glued Kevlar had the best compression properties, the Kevlar layer was further used in the bending and ballistic tests.

During the bending tests, it was also observed that the design of the sandwich structure influences the failure modes of the sandwich structures (Fig. 9, Table 3): the sandwich structures with only a foam core after reaching the maximal load significantly lost the load-bearing capacity, and the load fell to 1 kN. This is the result of breaking of the foam core via tensile cracks and subsequent foam compression under the Kevlar.

The second failure mode was observed when the ceramic was under the mesh; the strength is smaller in this case. It can be expected that the mesh on the compression side of the sandwich structure sample distributes the load to a significantly larger ceramic area, and then the load is transferred to the foam core, which effectively absorbs the energy.

In comparison to simple foam cores, the incorporation of mesh/ceramic into the foam core significantly improves the deflection at maximal load (Table 3). This indicates significant improvement in absorbed energy

PRE-PRINT ARTICLE
COPYRIGHT BY COMPOSITES THEORY AND PRACTICE JOURNAL
ISSN: 2299-128X

for the sandwich structure design. Among the different layer configurations, the highest energy absorption (area under the load-deflection curve) was exhibited by the following sandwich structure configuration: Kevlar-glue-steel mesh+foam-glue-foam+ceramic plate+steel mesh-glue-Kevlar. This configuration was further employed for the preliminary ballistic tests.

Note: The results are slightly biased by the different foam core densities in Fig. 9. The mechanical properties of the foams (modulus of elasticity [22], compression strength [23] and energy absorption capacity [24] depend on the foam density in a power law way. They decrease with decreasing density. Nevertheless, the S7 sample exhibited the best deflection at maximal load at the lowest foam core densities, thus indicating the best energy absorption capacity.

Table 3. Maximal bending load, strength and deflection at maximal load for investigated sandwich structure samples: K-Kevlar, S – steel mesh, F - foam.

No	Sandwich structure composition	F_{max}	y_{max}	σ_{max}	Areal weight
		[N]	**[mm]**	**[MPa]**	**[g/m^2]**
S1	K + F + F + K	3500	4.49	10.5	15600
S2	K + F + F + K	7220	4.41	20.4	16600
S3	K + S + F + F + Al_2O_3 + K	6780	**10.49**	20.0	20000
S4	K+ S + F + F + Al_2O_3 + S + K	5480	**8.99**	16.2	20800
S5	K+ S + F + F + S + Al_2O_3 + K	5280	7.84	16.1	20100
S6	K+ S + F + F + Al_2O_3 + K	5000	4.15	15.6	20500
S7	K+ S + F + F + Al_2O_3 + S + K	6160	**11.11**	19.0	21000
S8	K+ S + F + F + S + Al_2O_3 + K	5370	7.97	17.1	20200

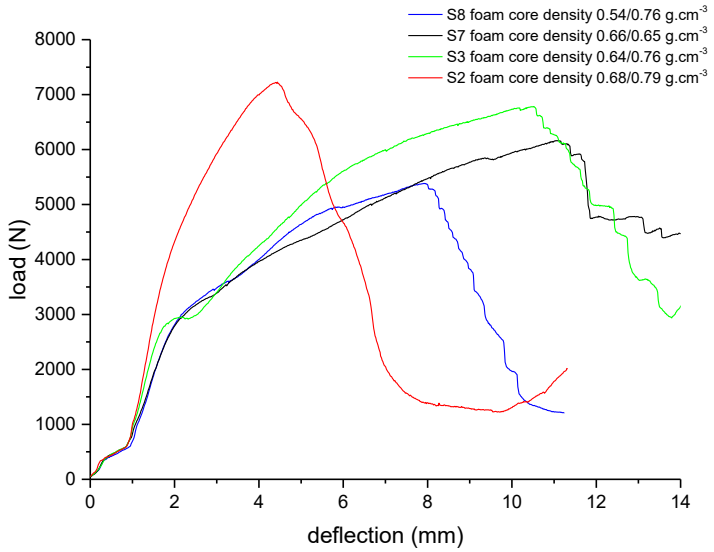

Fig. 9. Bending response of sandwich structure with Kevlar at various configurations of reinforcements: S2 – pure foam core, S3 – mesh +foam+ ceramic, S7 - mesh +foam+ ceramic+ mesh, S8 - mesh +foam + mesh + ceramic.

PRE-PRINT ARTICLE
COPYRIGHT BY COMPOSITES THEORY AND PRACTICE JOURNAL
ISSN: 2299-128X

Ballistic tests at the shot angle of 90° were performed on a sandwich structure sample mounted 20 mm above two joined pieces of aluminium plates (EN AW 7075); a total thickness of 24 mm. The bullet was stopped at the second aluminium plate; it was not penetrated (Fig. 10). Adiabatic plugging without complete penetration of the second plate was observed. The body of the projectile was destroyed during the tests. Almost no material loss was observed on the second aluminium plate.

The average depths of penetrated bullet *h* in the second plates are 19.2 and 22 mm for the tests only with EN AW 7075 aluminium alloy plates. In the case of the added sandwich structure, the depth in the second plate is only 16 mm, thus indicating that the sandwich structure shield absorbed some of the impact energy of the bullet. The kinetic energy of the bullet is $\frac{1}{2}\, mv^2 = \frac{1}{2}$ x 0.015 x 8332 = 5.2 J.

The ratio of energy absorbed by the added sandwich structure to the energy absorbed by only the EN AW 7075 aluminium alloy plates E_{sandw}/E_{AW7075} could be evaluated by cavity expansion theory [25,26].

Ductile hole enlargement (DHE) models [27], describe a primary failure mechanism when a hard, sharp-nosed projectile (such as an ogival or conical armour-piercing bullet) perforates monolithic aluminium plates like 7075-T6. Instead of fracturing cleanly via plugging, the target material flows radially outward to accommodate the incoming projectile shank. The work required to expand a hole from a zero initial radius to that of the penetrating projectile size is

$$W = \pi \cdot d^2/4 \cdot h_0 \cdot C \cdot \sigma \tag{1}$$

where d is the final diameter of the hole (i.e. the projectile calibre), h_0 is the initial thickness of the target, σ is the stress at the edge of the hole in the target material and depends on the used material, C is a constant referred to as the shape factor which defines the thickening at the edge of the expanded hole, $C = h/h_0$, where *h* is the depth of the penetration. In general, the work could be expressed as

$$W = \pi/4 \cdot \sigma \cdot h \cdot d^2 \tag{2}$$

Using Equation 2, the ratio of E_{sandw}/E_{AW7075} could be simply extracted as the ratio of h_{sandw}/h_{AW7075}. Considering the average value for an aluminium alloy bullet penetration depth of 20.6 mm, the energy ratio value is 16/20.6 = 0.777.

PRE-PRINT ARTICLE
COPYRIGHT BY COMPOSITES THEORY AND PRACTICE JOURNAL
ISSN: 2299-128X

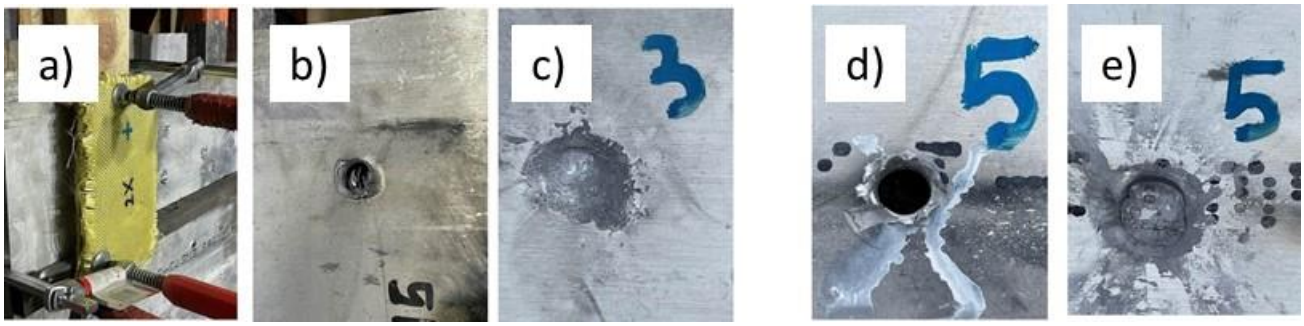

Fig. 10. Sandwich structure sample mounted 20 mm above EN AW 7075 aluminium plate after shooting at shot angle of 90°: a) front side of sandwich structure, b) rear side of 1st – aluminium plate below sandwich structure and c) front side of 2nd - aluminium plate below sandwich structure. For comparison, aluminium plates after the test without sandwich structure: d) rear side of 1st – aluminium plate, e) front side of 2nd - aluminium plate. Sandwich structure areal weight 23900 g/m^2.

This indicates that 23% of the bullet energy (1.19J) was absorbed by the developed sandwich structure secondary armour based on a sandwich structure made from aluminium foam. The result is promising for future work in this field.

Tests at the shot angle of 30° were also performed on the sandwich structure sample placed 20 mm above a 24 mm aluminium plate (EN AW 7075). The aluminium plate was not penetrated (Fig. 11). A ricochet effect inside the sandwich structure was observed in this case. Minor damage is visible on the aluminium plate; its deformation was less than 0.8 mm (Fig. 11, left). A single aluminium plate was also shot to compare the results: damage is visible on the aluminium plate, but it was not shot through either. Deformation of the aluminium plate is 3.5 mm in this case (Fig. 11, right). From the deformation size comparison, it is evident that the sandwich structure shield either absorbed some energy of the ricocheted bullet in comparison to the single plate or increased the angle of ricochet so that damage was avoided.

Morghode et al. [28] in their paper conducted a numerical study to analyse the ballistic performance of a layered configuration of Al_2O_3 and Al7075-T651 when impacted by a 7.62-mm APM2 bullet. At first, they found that a 20-mm-thick Al_2O_3 front plate with a 20-mm-thick Al 7075-T651 back plate successfully restricted the projectile. The area density of the armour was 133 kg/m^2. They found an optimal configuration at the thickness of the Al_2O_3 plate reduced to 18 mm and the Al 7075-T651 back plate thickness was reduced in steps to 10 mm. The area density for this combination was 97.22 kg/m^2.

PRE-PRINT ARTICLE
COPYRIGHT BY COMPOSITES THEORY AND PRACTICE JOURNAL
ISSN: 2299-128X

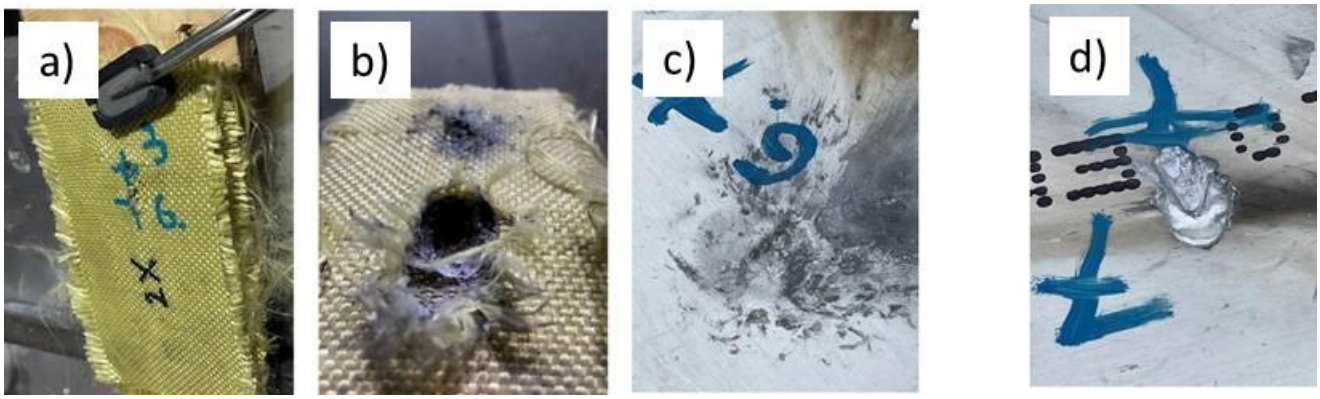

Fig. 11. Sandwich structure sample mounted 20 mm above EN AW 7075 aluminium plate after shooting at shot angle of 30°: a) front and b) rear side of sandwich structure, c) front side of aluminium plate below sandwich structure after the test. d) For comparison, aluminium plate after test without sandwich structure. Sandwich structure areal weight 23900 g/m^2.

Conclusions

Sandwich structures consisting of aluminium foams reinforced with a foamed-in stainless steel mesh, alumina ceramic plate or both, were prepared. As a cover sheet, Kevlar textile was glued onto the designed structure. Foams and reinforced foams used for the sandwich structure were prepared in the foam core density range of 0.53 – 0.91 g.cm^{-3}.

Modified compression tests were successfully developed and conducted using a pin simulating 7.62 mm calibre ammunition. The novelty of the design is that it is possible to deform the sample up to 100% strain since a densification region was not present on the stress-strain curve.

The reinforced foams with a ceramic plate or stainless-steel mesh are better than simple foams in compression strength and energy absorption at 100% strain. The glued alumina ceramic plate shows the best results due to better load distribution below the pin thanks to the glue, but there is a problem with broken ceramic and large pieces falling out after the test = failure against 2nd possible blast protection.

The sandwich structure composition with reinforced foam containing stainless steel mesh + an alumina ceramic plate on the top and glued Kevlar possesses the best compression strength, plateau stress and energy absorption at 100% strain among all the various reinforced foam and sandwich structure samples.

In the 3-point bending tests, the sandwich structures with only a foam core after reaching maximal load fail in tension at low deflection. They lost the energy absorption capacity as the load fell to 1 kN.

The incorporation of mesh/ceramic into the foam core significantly improves the deflection at maximal load, thus improving the absorbed energy for the sandwich structure design. From the different layer configurations, the highest energy absorption was observed for the following sandwich structure: Kevlar-glue-steel mesh+foam-glue-foam+ceramic plate+steel mesh-glue-Kevlar. Only this configuration was further used for the preliminary ballistic tests.

PRE-PRINT ARTICLE
COPYRIGHT BY COMPOSITES THEORY AND PRACTICE JOURNAL
ISSN: 2299-128X

The preliminary ballistic tests confirmed the validity of the multi-layered protection system concept. It was found that 23% of the bullet energy was absorbed inside the sandwich structures with reinforced aluminium foams. Nonetheless, further work is necessary to optimise the sandwich structure. It is recommended to vary the thickness of the ceramic layers, and to use better materials such as Kevlar, e.g. Dyneema or Endumax.

Funding

This work received funding from the Łukasiewicz Research Network-Institute of Non-Ferrous Metals, Poland - statutory work Project No. SUB/22/G/S/2024.

References

1. Directive (EU) 2022/2557 of the European Parliament and of the Council of 14 December 2022 on the resilience of critical entities and repealing Council Directive 2008/114/EC. Official Journal of the European Union. 2022 Dec 27;65(L 333):164–198.
2. EU-NATO Task Force on the Resilience of Critical Infrastructure. Final assessment report [Internet]. Brussels: European Commission/NATO; 2023 Jun [cited 2026 Aug 29]. Available from: nato.int.
3. National Consortium for the Study of Terrorism and Responses to Terrorism (START). Global Terrorism Database (1970–2020) [Internet]. College Park (MD): University of Maryland; 2022 [cited 2026 Aug 29]. Available from: https://www.start.umd.edu/gtd/
4. González-Jorge H, González-deSantos LM, Aldao E, Fontenla-Carrera G. C-UAS in the Protection of Critical Infrastructures. In: Carou D, Sartal A, Davim JP, editors. Applying Drones to Current Societal and Industrial Challenges. Cham: Springer; 2024. p. 131–153. https://doi.org/10.1007/978-3-031-55571-8_5
5. Langdon, G. S., Nurick, G. N., Balden, V. H., & Timmis, R. B. (2008). Perforated plates as passive mitigation systems. Defence Science Journal, 58(2), 238–247, 10.14429/dsj.58.1644.
6. Baloš S., Howard D., Brezulianu A., Labus Zlatanović D., Perforated Plate for Ballistic Protection—A Review, 2021, Metals, 2021, Vol. 11, 526, ISSN: 2075-4701 https://doi.org/10.3390/met11040526
7. Jiang JH, Xia CY, Yao J, Sun QK, Xia H. Vulnerability analysis of HSR bridge under near-field blast based on response surface method. Structures. 2023;58:105652. 10.1016/j.istruc.2023.06.053
8. Casas-Rodriguez JP, Calle JC, Robinson V, Maranon A. Cellular sandwich composites under blast loads. In: Silberschmidt V, editor. Dynamic Deformation, Damage and Fracture in Composite Materials and Structures. 2nd ed. Woodhead Publishing; 2023. p. 361-390. (Woodhead Publishing Series in Composites Science and Engineering). Available from: https://doi.org/10.1016/B978-0-12-823979-7.00014-4.
9. Pratomo A, Ruhma Z, Rukmono W, Martijanti, Sutarno S, Tse K. Ballistic Resistance Analysis of Hard Ceramic Combined with Aluminum Foam Sandwich Constructions. Int J Protective Struct. 2024. doi:10.1177/20414196241245126.

PRE-PRINT ARTICLE
COPYRIGHT BY COMPOSITES THEORY AND PRACTICE JOURNAL
ISSN: 2299-128X

10. Sarkhosh A, Mazaheri H, Kazemi M. Experimental and numerical study on ballistic resistance of aluminum foam sandwich panel considering porosity and dimensional effect. Int J Impact Eng. 2022;173:104441. DOI:10.1016/j.ijimpeng.2022.104441
11. Haro EE, Odeshi A, Castellanos S, Sanchez X, Abatta L, Criollo L, Alban A, Szpunar JA. Ballistic Impact Performance of Hybrid Composite Armors Made of Aluminum Foam Containing the Dispersion of Shear Thickening Fluid Made of Various Synthetic Nano-Fillers. Composites Part C: Open Access. 2023;12:100420. doi:10.1016/j.jcomc.2023.100420.
12. Brekken KA, Vestrum O, Dey S, Reyes A, Børvik T. Experimental Tests and Numerical Simulations on the Ballistic Impact Response of a Highly Inhomogeneous Aluminium Foam. Materials. 2022;15(13):4651.doi.org/10.3390/ma15134651
13. Kováčik J, Jerz J, Simančík F, Opálek A, Cantürk SB, Marșavina L, Linul E. Interplay between shape and composition in the compressive response of aluminum foams. Romanian Journal of Technical Sciences – Applied Mechanics. 2025;70(1-3):115-131. doi:10.59277/RJTS-AM.2025.1-3.07.
14. Linul E, Marşavina L, Linul PA, Kováčik J. Cryogenic and high temperature compressive properties of Metal Foam Matrix Composites. Composite Structures. 2019;209:490-498. doi:10.1016/j.compstruct.2018.11.006.
15. Jerz J, Simančík F, Bortel M, Kubo S, Kováčik J. The design of lightweight armour sheets. In: Banhart J, Fleck NA, editors. Cellular Metals and Metal Foaming Technology. Berlin: Metfoam; 2003.
16. Markaki AE. Mechanical Behaviour of Layered Metal Foam/Ceramic Composites [PhD thesis]. Cambridge: University of Cambridge; 2000.
17. Garcia-Avila M, Portanova M, Rabiei A. Ballistic performance of composite metal foams. Compos Struct. 2015;125:202–211. doi.org/10.1016/j.compstruct.2019.111032
18. Marx J, Portanova M, Rabiei A. A study on blast and fragment resistance of composite metal foams through experimental and modeling approaches. Compos Struct. 2015;194:652–661. doi.org/10.1016/j.compstruct.2018.03.075
19. DuPont. Kevlar® Technical Guide. E. I. du Pont de Nemours and Company. 2019
20. https://melkib.com/en_US/p/Melkib-MMA-Power-10-400ml-beige-2-component-methacrylic-adhesive-for-metal%2C-stainless-steel%2C-plastics%2C-composites%2C-balustrades%2C-very-durable%2C-cures-quickly%2C-resistant-to-impact%2C-weather-conditions/2922?srsltid=AfmBOoopPjr93qBYJyNWGczFcMtsUr40HgreGVgR-gpWawyi5hb77Cds - last accesses 29.08.2026
21. Simancik F, Rajner W, Laag R. Reinforced Alulight for structural use. In: Processing and properties of Lightweight Cellular Metals and Structures (TMS Annual Meeting), Seattle, 2002, p. 25.
22. Bădăluță AN, Galațanu SV, Kováčik J, Marșavina L. Multiscale modeling and optimization of aluminum foam material properties under dynamic load. Appl Sci. 2025;15(15):8433. doi:10.3390/app15158433.

PRE-PRINT ARTICLE
COPYRIGHT BY COMPOSITES THEORY AND PRACTICE JOURNAL
ISSN: 2299-128X

23. Kováčik J, Jerz J, Mináriková N, Marșavina L, Linul E. Scaling of compression strength in disordered solids: metallic foams. Frattura ed Integrità Strutturale. 2016;10(36):55-62. doi:10.3221/IGF-ESIS.36.06.
24. Galațanu SV, Marșavina L, Kováčik J, Linul E. Influence of density and loading speed on static and impact properties of closed-cell metallic foams. Eng Fail Anal. 2024;161:108297. doi:10.1016/j.engfailanal.2024.108297.
25. Bishop RF, Hill R, Mott NF. The theory of indentation and hardness testing. Proc Phys Soc. 1945;57(3):147-157.
26. Forrestal MJ, Warren TL. Perforation equations for conical and ogival nose rigid projectiles into aluminum target plates. Int J Impact Eng. 2009;36(2):220-225. doi:10.1016/j.ijimpeng.2008.04.005.
27. Ryan S, Nguyen LH, Gallardy D, Cimpoeru SJ. A scaling law for predicting the ballistic limit of aluminium alloy targets perforated in ductile hole formation. Int J Impact Eng. 2018;116:34-50. doi:10.1016/j.ijimpeng.2018.02.005.
28. Morghode DS, Thakur DG, Salunkhe S, Cepova L, Abouel Nasr E. Numerical study on the optimized thickness of layer configuration against the 7.62 APM2 projectile. Front Mech Eng. 2024;10:1322640. doi:10.3389/fmech.2024.1322640